Terra Nova

doi: 10.1111/ter.12022

Revisiting the orogenic energy balance in the western Taiwan orogen with weak faults

Brendan J. Meade

Department of Earth and Planetary Sciences, Harvard University, Cambridge MA, 02138, USA

ABSTRACT

Orogens at convergent margins must meet the energetic requirements necessary to lift rocks against gravity, allow for frictional sliding along basal detachments and accommodate internal deformation processes. The combination of critical taper and kinematic wedge theories predicts the partitioning between these energy sinks as a function of both fault and crustal strengths. Integrating contemporary estimates of both crustal pore fluid pressures and the coefficient of friction on major faults, we find that work associated with internal deformation processes is the dominant energy sink in the western Taiwan orogenic wedge. These processes consume 54% of the total work budget, while the dissipation rates associated with frictional sliding on the basal detachment and lifting rocks against gravity are lower, requiring only 11% and 35% respectively. These results suggest a mechanical dichotomy in orogenic wedges where the faulting dominates the kinematic deformation budget, but internal distributed deformation processes dominate the energy budget.

Terra Nova, 25, 160–164, 2013

Introduction

At tectonically active margins, fold-and-thrust belts such as the Himalaya, sub-Andes and Taiwan orogens are marked by high crustal strain rates accommodating a range of deformation processes. The energy balance in these compressive orogens has been a subject of interest both for identifying the most energetically expensive deformation processes (Elliott, 1976; Dahlen, 1988) and for assessing whether or not orogens evolve in accordance with a minimum work principle (e.g. Masek and Duncan, 1998; Maillot and Leroy, 2003; Cooke and Murphy, 2004; Ismat and Mitra, 2005; Del Castello and Cooke, 2007). In addition, quantifying energy partitioning within an orogen is important for developing mechanically consistent models that satisfy the energy balance in addition to the more commonly considered momentum and mass balances. A range of processes may dissipate energy within an actively deforming fold-and-thrust belt, including work done lifting rocks against gravity, frictional resistance to sliding on a basal detachment, fracture propagation, pressure solution, internal faulting and folding. To understand the partitioning of work into these energy sinks, and the role of internal deformation processes in particular, two approaches have been adopted: (1) the mechanical analysis of specific individual internal deformation processes (Mitra and Boyer, 1986; Cooke and Murphy, 2004; Ismat and Mitra, 2005; Del Castello and Cooke, 2007); and (2) the inference of internal dissipation rates from an orogen-wide energy balance perspective (Elliott, 1976; Barr and Dahlen, 1988; Dahlen, 1988). Here, we adopt the second approach based on simple mechanical models and consider the strain budgets associated with candidate deformation processes to constrain upper crustal viscosity and determine whether faulting not only dominates the strain rate budget but also serves as the most energetically expensive step in orogen growth.

Correspondence: Brendan Meade, Department of Earth and Planetary Sciences, Harvard University, 20 Oxford Street, Cambridge, MA 02138, USA. Tel.: 6174958921; e-mail: meade@fas.harvard.edu

Revisiting energy partitioning in the Taiwan orogen

Energy partitioning inside of an actively deforming orogen can be determined at mass-flux steady state, where the rate of tectonic influx is equal to erosional efflux (Barr and Dahlen, 1988; Dahlen, 1988), and the rate of work done on the orogen by tectonic forces, $\dot{W}_T$, is balanced by the rate of energy dissipation from (1) frictional slip on the basal detachment, $\dot{W}_D$, (2) lifting material against gravity, $\dot{W}_G$, and (3) accommodation of deformation processes internal to the orogenic wedge, $\dot{W}_I$. We calculate $\dot{W}_T$, $\dot{W}_D$ and $\dot{W}_G$ by combining scale-invariant critical taper wedge theory (Dahlen, 1984) with scale-dependent homogeneous pure shear wedge kinematics (e.g. Chapple, 1978; Dahlen, 1988), which are consistent with rock exhumation pathways inferred from analogue experiments (e.g. Konstantinovskaia and Malavieille, 2005) and modelling of thermochronologic data (e.g. Willett and Brandon, 2002).

Utilizing critical taper wedge theory Dahlen (1988) showed that the tectonic work rate on an orogenic wedge is given by the horizontal compressive stress integrated over the height over which it is supported, $\dot{W}_T = \rho g \Lambda V H^2/2$ (W/m along strike), with, $\Lambda = 1 + [2(1 - \lambda_i) \sin(\tan^{-1}\mu_i)]/[1 - \sin(\tan^{-1}\mu_i)]$ where ρ is the density of crustal rocks, g is the acceleration of gravity, V is the convergence velocity, H is the height of the thickest part of the orogenic wedge, λ_i is the ratio of pore fluid to lithostatic pressure in the orogenic wedge and μ_i is the internal coefficient of friction. The tectonic work rate depends linearly on wedge cross-sectional area and may range from 3 to 25 kW m^{-1} along strike in western Taiwan (Table 1). The wide range in work rate values emerges from different interpretations of the

Table 1 Summary of differences in material properties and wedge geometry used for critical taper energy-partitioning calculations (§Dahlen, 1988; †Suppe, 2007; ‡Yue, 2007; *Yu *et al.*, 1997). Material properties assumed throughout are as follows: $\rho = 2500$ kg m^{-3}, $\mu_i = 0.8$, and $\lambda_b = 0.7$. Variable material properties are the coefficient of friction on the basal detachment, μ_b, and the ratio of pore fluid to lithostatic pressure in the crust λ_i. Variable geometric properties are the mean topographic slope α, the dip of the basal detachment β and the thickness of the incoming material at the toe of the wedge h (Fig. 1). Case 2 is the more localized area described in this article. The lower three rows show the normalized work partitioning percentages with the shaded regions indicating the largest energy sink in each case.

	Case 1§	Case 2
μ_b	0.70	0.27†
λ_i	0.7	0.4‡
α	3.0°	2.0°†
β	6.0°	2.7°†
h	7 km	5 km†
W	90 km	40 km†
V	70 mm a^{-1}	40 mm a^{-1}*
$\dot{W}_T$	24 kW m^{-1}	3 kW m^{-1}
$\dot{W}_I/\dot{W}_T$	16%	54%
$\dot{W}_G/\dot{W}_T$	39%	35%
$\dot{W}_D/\dot{W}_T$	45%	11%

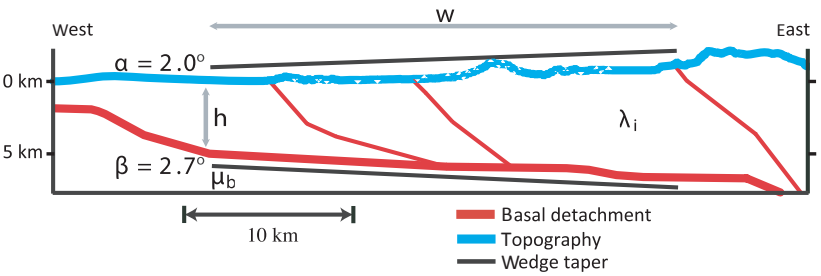

Fig. 1 Schematic cross-section of the western Taiwan fold-and-thrust belt and relation to critical taper wedge theory parameters (at ~24°N latitude, after Suppe, 2007). Continental material of thickness h is accreted from the east margin into the wedge of width w, which slips above the Chinshui Shale detachment (thick red line) with a coefficient of friction, μ_b. The taper (angle between thin black lines) of the orogen is the sum of the mean topographic slope, α, and detachment dip, β. The ratio of pore fluid to lithostatic pressure in upper crustal rocks is given by, λ_i.

Taiwan wedge: treating the entire western side of Taiwan as the orogenic wedge corresponds to high work rate values (Barr and Dahlen, 1988; Dahlen, 1988), but limiting the critical taper wedge model to a 40-km-wide foothill region in the vicinity of the Chelungpu fault (Suppe, 2007) gives work rate values that are an order of magnitude smaller (Fig. 1, Table 1). The rest of the paper is focused on this foothill region where sufficient data are available on material properties, wedge geometry and fault kinematics.

The fractional work rates required for frictional sliding on the basal detachment, and against gravity are $\dot{W}_D/\dot{W}_T = 1/[(\beta + \Lambda h/w)/\{(1-\lambda_b)\mu_b\} + 1]$ and $\dot{W}_G/\dot{W}_T = (\beta + h/w)/[\beta + (1-\lambda_b)\mu_b + \Lambda h/w]$, respectively, where λ_b is the ratio of pore fluid to lithostatic pressure on the basal detachment, μ_b is the coefficient of friction on the basal detachment, β is the dip of the basal detachment, h is the thickness of the accreting layer at the toe of the orogenic wedge and w is the width of the orogenic wedge (Dahlen, 1988). In contrast, the work associated with individual internal deformation processes is more difficult to quantify because the spatial extent of candidate processes (e.g. pressure solution, fracture propagation, internal faulting, bending, bedding plane slip) is generally obscured at depth in active mountain belts. Elliott (1976) recognized this problem and used an energy balance approach to solve for the work associated with internal deformation that neglected tectonic stress, $\dot{W}_T = 0$, and assumed $\dot{W}_G$ was an energetic source rather than sink (i.e. gravity sliding hypothesis). Similarly, Dahlen (1988) used critical taper wedge theory and pure shear deformation models to solve for the total amount of work associated with internal deformation as:

$$\dot{W}_I = \dot{W}_T - (\dot{W}_D + \dot{W}_G).$$

Applied to the westward side of the Taiwan orogen and assuming $V = 70$ mm a^{-1} with an orogen width of 90 km, Dahlen (1988) estimated work against frictional sliding on the basal detachment and against gravity dissipate 46% and 39%, respectively, of the total work done on the orogen (Table 1). Internal deformation processes are the least energetically expensive step, consuming only 16% of the total work budget (Dahlen, 1988). These calculations assumed that the basal detachment is strong, characterized by a coefficient of friction $\mu_b = 0.7$, and that the wedge is effectively weak because pore fluid pressures are close to lithostatic, $\lambda_i = 0.7$.

More recently, estimates of wedge geometry and material properties have been revised based on new observations and model inferences (Table 1). Structural interpretations of seismic reflection data and precise earthquake locations suggest that wedge taper in the vicinity of the Chelungpu fault in western Taiwan is 4.7° (Fig. 1) (Suppe, 2007), approximately 50% less than that previously assumed (Dahlen, 1988). This shallower wedge taper, defined over a 40-km-wide region, implies a weak basal detachment (at the depth of the Chinshui Shale) with a coefficient of friction $\mu_b < 0.3$, neglecting cohesive strength and assuming $\lambda_b = 0.7$. In addition, analysis of sonic logs in western Taiwan has suggested that the ratio of pore fluid to lithostatic pressures at depths <6 km is close to hydrostatic, $\lambda_i = 0.4$ (Yue, 2007), rather than the $\lambda_i = 0.7$ value previously assumed (Table 1). Using these material parameters, and a geodetically constrained shortening rate of 40 mm a^{-1} (Yu *et al.*, 1997), we calculate that the work rate due to sliding on the basal detachment is 18% of the total work rate budget. Internal deformation processes consume 47% (~2 kW m^{-1}), the largest fraction of total work dissipation (Table 1, Fig. 2). More generally, the internal deformation work rate is the largest source of dissipation for basal detachment coefficients of friction

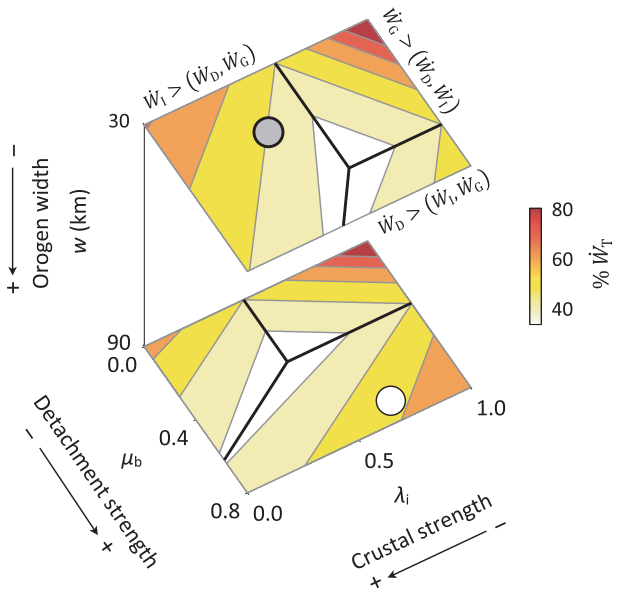

Fig. 2 Energy-partitioning phase diagram. Work done on the orogenic wedge, $\dot{W}_T$, is balanced by work against gravity, $\dot{W}_G$, frictional sliding on the basal detachment, $\dot{W}_D$, and that associated with internal deformation processes $\dot{W}_I$. Reasonable variations in orogen width, w, basal detachment coefficient of friction, μ_b, and the ratio of pore fluid to lithostatic pressure in crustal rocks, λ_i, give rise to different energy-partitioning solutions with different dominant mechanisms. Thick black lines denote the boundaries between the three regimes where $\dot{W}_G$, $\dot{W}_D$, or $\dot{W}_I$ dominate and coloured contours give the percentage of the total work budget dissipated by the most energetically expensive process. The white circle is the classic Dahlen (1988) solution with a weak crust, $\lambda_i = 0.7$, and strong basal detachment, $\mu_b = 0.7$, (case 1, in Table 1) where work against frictional sliding on the basal detachment dominates, $\dot{W}_D > (\dot{W}_I, \dot{W}_G)$, and the grey circle is the solution with weak basal detachment $\mu_b = 0.27$ and a strong crust $\lambda_i = 0.4$ (case 2, in Table 1) where work associated with internal deformation processes dominates, $\dot{W}_I > (\dot{W}_D, \dot{W}_G)$. All calculations assume $\rho = 2500$ kg m^{-3}.

$\mu_b < 0.45$ with $\lambda_i = 0.4$ and $\lambda_b = 0.7$. However, while $\dot{W}_I$ is dominant in this case, it is only the combination of both the pore fluid pressure and basal detachment friction estimates that lead to this conclusion; alone neither is sufficient (Fig. 2). If pore fluid pressures inside the wedge were 70–100% of lithostatic pressure, the crust would be weaker, and $\dot{W}_G$ would dominate the work rate budget despite the weakness of the basal detachment (Fig. 2).

Energetics of candidate internal deformation processes

The inference that the Chinshui Shale detachment is weak (Suppe, 2007), characterized by a coefficient of friction <50% of the Byerlee (1978) value, is consistent with laboratory experiments (e.g. Di Toro *et al.*, 2004), and heat flow measurements in active tectonic environments (e.g. Lachenbruch and Sass, 1980; Barr and Dahlen, 1990). However, the source of the energy required for deformation processes interior to the Taiwan orogenic wedge (a minimum $\dot{W}_I \sim 2$kW m^{-1}, for the narrowest critical taper wedge interpretation, Table 1) is less well understood, and in particular, it is difficult to constrain the spatial extent over which processes such as frictional slip on internal faults, fracture creation, pressure solution and Coble creep operate. To understand the relative importance of each of these processes as energetic sinks, we consider each individually as a simple thought experiment. Frictional slip on faults requires a work rate of $\mu(1 - \lambda_i)\bar{\sigma}vl$, where $\bar{\sigma}$ is the mean normal stress on a fault of length, l slipping at rate, v. Taking the Chelungpu fault (Fig. 1) as an example of an active fault within the west Taiwan orogenic wedge, slipping at a rate of ~15 mm a^{-1} (Simoes *et al.*, 2007), gives a dissipation rate of 0.05 kW m^{-1} along strike assuming a Byerlee coefficient of friction, $\mu = 0.85$, as an upper bound and hydrostatic pore fluid pressure. This dissipation rate is lower than that associated with the basal detachment because faults interior to the wedge slip at slower rates and are subjected to lower normal stresses at shallow crustal depths. In order for frictional sliding on faults within the orogenic wedge to account for the entirety of $\dot{W}_I$ would require ~20 structures similar to the Chelungpu, which would be inconsistent with geodetic observations suggesting the shortening rate across western Taiwan is limited to ~40 mm a^{-1} (Yu *et al.*, 1997) and which we assume to be constant in time. Creation of new fracture surfaces will also contribute to $\dot{W}_I$ when differential stress exceeds rock strength. While mode I fractures are the less energetically expensive, mode III cracks may be formed in compressive environments with experimentally determined fracture energies ranging from 0.3 to 5.1 kJ m^{-2} at upper crustal confining pressures (Wong, 1982). If fracture creation alone were to account for all internal dissipation, the rate of fracture length created per unit metre along orogen strike would be $\dot{l} = \dot{W}_I/G \approx 0.3$ m s^{-1}. This prediction may be difficult to test because significant fracture area could be accommodated in densely fractured regions, where fault system geometry is characterized by fractal dimension as high as 1.6 (e.g. Hirata, 1989).

Ductile deformation processes, including pressure solution and Coble creep, dissipate energy at a rate $\sigma\,\dot{\epsilon}_v\,A$ per unit metre along strike, where $\dot{\epsilon}_v$ is the ductile strain rate. An upper bound on $\dot{\epsilon}_v$ can be determined from the relationship between geologically determined fault slip rates and geodetic observations of interseismic deformation. Geodetically measured interseismic strain rates in western Taiwan are generally consistent with earthquake cycle models based on geologically inferred fault slip rates. Strath terraces uplifted near the Chelungpu (Fig. 1) and nearby Chushiang faults suggest

Holocene slip rates of 12.9 ± 4.8 mm a^{-1} and 2.9 ± 1.6 mm a^{-1}, respectively (Simoes *et al.*, 2007), within the range of 15.1–20.5 mm a^{-1} estimated from geodetically constrained elastic block models that represent both faults as a single eastward dipping structure (Ching *et al.*, 2011). This similarity suggests that the majority of geodetically measured strain is likely to result from recoverable elastic deformation rather than permanent ductile deformation. While the two slip rate estimates agree within uncertainties, this would also be the case if $\dot{\epsilon}_v$ accounted for as much as ~25% of the geodetically observed 10^{-14} s^{-1} strain rate (Hsu *et al.*, 2008). Thus, the viscous strain rate can be as large as $\dot{\epsilon}_v = 2.5 \times 10^{-15}$ s^{-1} without the total strain rate budget exceeding the upper bound from geodetic observations or degrading the agreement between geological and geodetic fault slip rate estimates. Assuming a linear viscous rheology and that viscous deformation processes account for all internal wedge dissipation, an average upper crustal viscosity can be estimated as: $\eta = \dot{W}_I/\dot{\epsilon}_v^2 A = 2.4 \times 10^{24}$ Pa s (Fig. 3). Because the wedge model is applied to the shallowest and coolest part of the crust, the likely active viscous deformation process is pressure solution rather than Coble creep, which is activated at temperatures exceeding $T = 350$ °C (e.g. McClay, 1977). Pressure solution deformation, the diffusive dissolution and reprecipitation of mineral phases through narrow aqueous films at grain boundaries, can be active at upper crustal strain rates and temperatures with grain sizes, $d = (32\sigma_a V_m C_0 D_b w_b/\dot{\epsilon}_v \rho RT)^{1/3}$ of ~5 μm (Fig. 3) at an applied stress, σ_a, of 100 MPa (Rutter, 1976). Material parameters, estimated for calcite and granite, are as follows: the molar volume of the crystalline solid, $V_m = 3.12 \times 10^{-10}$ m^3 mol^{-1}; the concentration of saturated solution at grain boundaries, $C_0 = 400$ kg m^{-3}; the grain boundary diffusivity, $D_b = 4 \times 10^{-20}$ m^2 s^{-1}; the effective grain boundary width, $w_b = 2$ nm; and R is the gas constant (Rutter, 1976). If active pressure solution, or Coble creep at greater depths in Taiwan (Beyssac *et al.*, 2007), only occurs in more localized regions, the mean grain size in the ductile process zones may be larger, and the effective upper crustal viscosity higher.

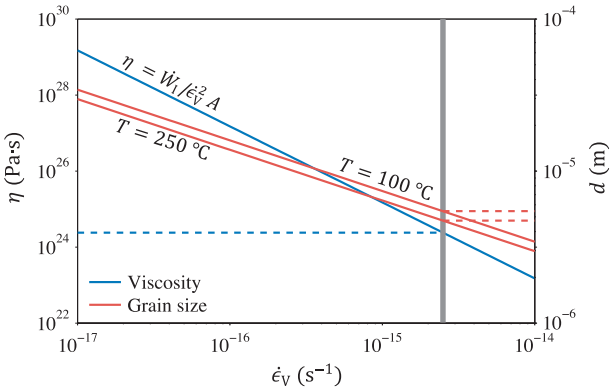

Fig. 3 Upper crustal viscosity (solid blue line) and characteristic grain size (solid red lines) for homogeneously distributed pressure solution flow as a function of viscous strain rate. Values of viscosity and grain size consistent with both the internal dissipation rate and an upper bound to the strain rate (vertical grey line, $\dot{\epsilon}_v = 2.5 \times 10^{-15}$) associated with viscous processes in the western Taiwan orogenic wedge are shown as dashed lines.

Discussion

All three of the candidate energetic sinks (frictional sliding on faults internal to the orogenic wedge, fracture creation and pressure solution) likely act within the western Taiwan foothills. Simple models of diffuse pressure solution alone with an upper crustal viscosity exceeding 10^{24} Pa s appear consistent with both geodetic strain rate observations and the orogen-wide energy balance. The hypothesis that diffuse deformation of highly viscous upper crust requires more energy than does frictional sliding on faults is complementary to the inference of weak major faults within a strong crust in western Taiwan (Suppe, 2007). Over geological time, deformation of the orogenic wedge requires that the relative work budget requirements for all dissipation sources be met, so that these processes may be considered coupled rather than independent (e.g. Elliott, 1976). For the fold-and-thrust belt case, the deformation associated with any dissipative process ($\dot{W}_G/\dot{W}_T, \dot{W}_D/\dot{W}_T, \dot{W}_I/\dot{W}_T$) cannot occur unless the energetic requirement for the most expensive dissipation source is also met (e.g. $\dot{W}_I/\dot{W}_T$ for the case of the western Taiwan foothills). In other words, a dichotomy may exist within the Taiwan orogen: distributed deformation of a high viscosity, or densely fractured, upper crust may dominate the energy budget, but the majority of geodetically and geologically observed strain may be accommodated by relatively energetically efficient faulting. Whether or not this is the case for other orogenic wedges will require not only an assessment of wedge geometries and material properties but also characterizations of fault slip rates above the basal detachment, making it challenging to test this theory at submarine wedges. Studies of other orogenic wedges may also reveal cases where work rates are equipartitioned, $\dot{W}_G/\dot{W}_T = \dot{W}_D/\dot{W}_T = \dot{W}_I/\dot{W}_T$, so that there may be no uniquely identifiable rate-limiting process.

References

Barr, T.D. and Dahlen, F.A., 1988. Thermodynamic efficiency of brittle frictional mountain building. *Science*, **242**, 749–752.

Barr, T.D. and Dahlen, F.A., 1990. Constraints on friction and stress in the Taiwan fold-and-thrust belt from heat flow and geochronology. *Geology*, **18**, 111–115.

Beyssac, O., Simoes, M., Avouac, J.P., Farley, K.A., Chen, Y.-G., Chan, Y.-C. and Goffe, B., 2007. Late Cenozoic metamorphic evolution and exhumation of Taiwan. *Tectonics*, **26**, TC6001.

Byerlee, J., 1978. Friction of rocks. *Pure Appl. Geophys.*, **116**, 615–626.

Chapple, W.M., 1978. Mechanics of thin-skinned fold-and-thrust belts. *Bull. Geol. Soc. Am.*, **89**, 1189–1198.
Ching, K.-E., Rau, R.-J., Johnson, K.M., Lee, J.-C. and Hu, J.-C., 2011. Present-day kinematics of active mountain building in Taiwan from GPS observations during 1995–2005. *J. Geophys. Res.*, **116**, B08406.
Cooke, M. and Murphy, S., 2004. Assessing the work budget and efficiency of fault systems using mechanical models. *J. Geophys. Res.*, **109**, B10408.
Dahlen, F.A., 1984. Noncohesive critical Coulomb wedges – an exact solution. *J. Geophys. Res.*, **89**, 125–133.
Dahlen, F.A., 1988. Mechanical energy budget of a fold-and-thrust belt. *Nature*, **331**, 335–337.
Del Castello, M. and Cooke, M., 2007. Underthrusting–accretion cycle: work budget as revealed by the boundary element method. *J. Geophys. Res.*, **112**, B12404.
Di Toro, G., Goldsby, D.L. and Tullis, T. E., 2004. Friction falls towards zero in quartz rock as slip velocity approaches seismic rates. *Nature*, **427**, 436–438.
Elliott, D., 1976. Energy balance and deformation mechanisms of thrust sheets. *Phil. Trans. Roy. Soc. London*, **283**, 289–312.
Hirata, T., 1989. Fractal dimension of fault systems in Japan: fractal structure in rock fracture geometry at various scales. *Pure Appl. Geophys.*, **131**, 157–170.
Hsu, Y.-J., Yu, S.-B., Simons, M., Kuo, L.-C. and Chen, H.-Y., 2008. Interseismic crustal deformation in the Taiwan plate boundary zone revealed by GPS observations, seismicity, and earthquake focal mechanisms. *Tectonophysics*, **479**, 4–18.
Ismat, Z. and Mitra, G., 2005. Fold–thrust belt evolution expressed in an internal thrust sheet. Sevier orogen: the role of cataclastic flow. *Bull. Geol. Soc. Am.*, **117**, 764–782.
Konstantinovskaia, E. and Malavieille, J., 2005. Erosion and exhumation in accretionary orogens: experimental and geological approaches. *Geochem. Geophys. Geosyst.*, **6**, Q02006.
Lachenbruch, A.H. and Sass, J.H., 1980. Heat flow and energetics of the San Andreas fault zone. *J. Geophys. Res.*, **85**, 6185–6223.
Maillot, B. and Leroy, Y.M., 2003. Optimal dip based on dissipation of back thrusts and hinges in fold-and-thrust belts. *J. Geophys. Res.*, **108**, 2320.
Masek, J.G. and Duncan, C.C., 1998. Minimum-work mountain building. *J. Geophys. Res.*, **103**, 907–917.
McClay, K.R., 1977. Pressure solution and Coble creep in rocks and minerals: a review. *J. Geol. Soc. London*, **134**, 57–70.
Mitra, G. and Boyer, S.E., 1986. Energy balance and deformation mechanisms of duplexes. *J. Struct. Geol.*, **8**, 291–304.
Rutter, E.H., 1976. The kinetics of rock deformation by pressure solution. *Phil. Trans. Roy. Soc. London*, **283**, 203–219.
Simoes, M., Avouac, J.P. and Chen, Y.-G., 2007. Slip rates on the Chelungpu and Chushiang thrust faults inferred from a deformed strath terrace along the Dungpuna river, west central Taiwan. *J. Geophys. Res.*, **112**, B03S10.
Suppe, J., 2007. Absolute fault and crustal strength from wedge tapers. *Geology*, **35**, 1127–1130.
Willett, S.D. and Brandon, M.T., 2002. On steady states in mountain belts. *Geology*, **30**, 175–178.
Wong, T.-F., 1982. Shear fracture energy of Westerly granite from post failure behavior. *J. Geophys. Res.*, **87**, 990–1000.
Yu, S.B., Chen, H.Y. and Kuo, L.C., 1997. Velocity field of GPS stations in the Taiwan area. *Tectonophysics*, **274**, 41–59.
Yue, L.F., 2007. Active structural growth in central Taiwan in relationship to large earthquakes and pore-fluid pressures. Unpubl. doctoral dissertation, Princeton University, 262 pp.

Received 16 August 2012; revised version accepted 27 November 2012

